Arthritis & Rheumatology
Vol. 71, No. 10, October 2019, pp 1681–1690
DOI 10.1002/art.40931

American College of Rheumatology
Empowering Rheumatology Professionals

Inhibition of EZH2 Ameliorates Lupus-Like Disease in MRL/*lpr* Mice

Dallas M. Rohraff,[1] Ye He,[2] Evan A. Farkash,[1] Mark Schonfeld,[1] Pei-Suen Tsou,[1] and Amr H. Sawalha[3]

Objective. We previously identified a role for EZH2, a transcriptional regulator in inducing proinflammatory epigenetic changes in lupus CD4+ T cells. This study was undertaken to investigate whether inhibiting EZH2 ameliorates lupus-like disease in MRL/*lpr* mice.

Methods. EZH2 expression levels in multiple cell types in lupus patients were evaluated using flow cytometry and messenger RNA expression data. Inhibition of EZH2 in MRL/*lpr* mice was achieved by intraperitoneal 3′-deazaneplanocin (DZNep) administration using a preventative and a therapeutic treatment model. Effects of DZNep on animal survival, anti–double-stranded DNA (anti-dsDNA) antibody production, proteinuria, renal histopathology, cytokine production, and T and B cell numbers and percentages were assessed.

Results. EZH2 expression levels were increased in whole blood, neutrophils, monocytes, B cells, and CD4+ T cells in lupus patients. In MRL/*lpr* mice, inhibition of EZH2 by DZNep was confirmed by significant reduction of EZH2 and H3K27me3 in splenocytes. Inhibiting EZH2 with DZNep treatment before or after disease onset improved survival and significantly reduced anti-dsDNA antibody production. DZNep-treated mice displayed a significant reduction in renal involvement, splenomegaly, and lymphadenopathy. Lymphoproliferation and numbers of double-negative T cells were significantly reduced in DZNep-treated mice. Concentrations of circulating cytokines and chemokines, including tumor necrosis factor, interferon-γ, CCL2, RANTES/CCL5, interleukin-10 (IL-10), keratinocyte-derived chemokine/CXCL1, IL-12, IL-12p40, and CCL4/macrophage inflammatory protein 1β, were decreased in DZNep-treated mice.

Conclusion. EZH2 is up-regulated in multiple cell types in lupus patients. Therapeutic inhibition of EZH2 abrogates lupus-like disease in MRL/*lpr* mice, suggesting that EZH2 inhibitors may be repurposed as a novel therapeutic option for lupus patients.

INTRODUCTION

Systemic lupus erythematosus (SLE), or lupus, is a chronic relapsing autoimmune disease that involves multiple organ systems. Lupus is characterized by the production of autoantibodies directed against nuclear antigens and a dysregulated immune response. The etiology of lupus remains unknown, although both genetic and epigenetic mechanisms have been shown to contribute to disease pathogenesis (1,2).

DNA methylation plays a critical role in the pathogenesis of lupus (3). Abnormal DNA methylation patterns have been described in multiple immune cell types isolated from lupus patients, and a role for genetic–epigenetic interaction in the pathogenesis of lupus has been suggested (4). Furthermore, abnormal DNA methylation patterns in lupus have been shown to contribute to clinical heterogeneity, disease variability between ethnicities, and lupus flare and remission (4).

EZH2 induces H3K27me3 and is the catalytic component of the highly conserved polycomb regressive complex 2. Our group previously demonstrated that increased disease activity in lupus patients is characterized by an early epigenetic shift in naive CD4+ T cells that precedes CD4+ T cell differentiation and effector T cell transcriptional activity (5). We provided evidence that this epigenetic shift is likely induced by EZH2 overexpression as a result of down-regulation of microRNA-101 (miR-101) and miR-26a, in addition to showing that EZH2 overexpression mediates increased T cell adhesion in lupus due to EZH2-induced demethylation and transcrip-

Supported by the Lupus Research Alliance and the National Institute of Allergy and Infectious Diseases (NIAID), NIH (grant R01-AI-097134). Dr. Farkash's work was supported by the NIAID, NIH (grant K23-AI-108951).

[1]Dallas M. Rohraff, BSc, Evan A. Farkash, MD, PhD, Mark Schonfeld, BSc, Pei-Suen Tsou, PhD: University of Michigan, Ann Arbor; [2]Ye He, BSc: University of Michigan, Ann Arbor, and the Second Xiangya Hospital and Central South University, Changsha, China; [3]Amr H. Sawalha, MD: University of Michigan, Ann Arbor, and University of Pittsburgh, Pittsburgh, Pennsylvania.

No potential conflicts of interest relevant to this article were reported.

Address correspondence to Amr H. Sawalha, MD, UPMC Children's Hospital of Pittsburgh, Division of Rheumatology, University of Pittsburgh, 4401 Penn Avenue, Rangos Research Center, Room 7123, Pittsburgh, PA 15224. E-mail: asawalha@pitt.edu.

Submitted for publication December 18, 2018; accepted in revised form May 14, 2019.

tional derepression of the junctional adhesion molecule A (JAM-A) (5,6).

EZH2 overexpression has been linked to increased invasiveness in a number of malignancies, and EZH2 inhibitors are currently being evaluated in clinical trials for cancer therapy (7). Our findings indicate that inhibiting EZH2 might have therapeutic potential in lupus, suggesting the possibility of pharmacologic repurposing of EZH2 inhibitors as a therapeutic option. In this study, we first examined EZH2 expression patterns in other immune cell types isolated in the peripheral blood from lupus patients. We then tested the effects of using 3′-deazaneplanocin (DZNep), an EZH2 inhibitor, in the lupus-prone MRL/*lpr* mouse model. DZNep is an S-adenosylhomocysteine hydrolase inhibitor that inactivates methyltransferase activity through feedback inhibition by accumulation of S-adenosylhomocysteine (8). DZNep has also been shown, by us and others, to decrease EZH2 levels (6,7). In the current study, we utilized both preventative and therapeutic approaches of administering DZNep to MRL/*lpr* mice. Our findings provide robust preclinical evidence supporting the potential use of EZH2 inhibitors in lupus, paving the way for repurposing EZH2 inhibitors in clinical trials.

MATERIALS AND METHODS

EZH2 expression in B cells, monocytes, and neutrophils in lupus patients. We recruited a total of 6 lupus patients (mean ± SEM age 46.2 ± 5.4 years, range 32–61 years) and 6 healthy controls (mean ± SEM age 44.5 ± 5.8 years, range 30–63 years). All lupus patients fulfilled the American College of Rheumatology classification criteria for SLE (9). The mean SLE Disease Activity Index score (10) score for lupus patients was 2, with a median of 1 (range 0–6) (see Supplementary Table 1, on the *Arthritis & Rheumatology* web site at http://onlinelibrary.wiley.com/doi/10.1002/art.40931/abstract). Lupus patients receiving cyclophosphamide or methotrexate were excluded from the study. All subjects provided written informed consent approved by the Institutional Review Board of the University of Michigan.

Peripheral whole blood was collected from each study subject, and erythrocytes in blood samples were lysed with RBC Lysis Buffer (eBioscience). Remaining whole blood cells were incubated with Human Seroblock (Bio-Rad) in Cell Staining Buffer (BioLegend) to block nonspecific Fc receptor binding of Ig, and extracellularly stained with the following antibodies: allophycocyanin (APC)–Cy7–conjugated anti-CD14 (clone 63D3; BioLegend), phycoerythrin (PE)–conjugated mouse anti-human CD16b (clone CLB-gran11.5; BD Biosciences), and APC-conjugated anti-CD19 (clone HIB19; BioLegend). Afterward, cells were fixed with Fixation Buffer (BioLegend), permeabilized with Intracellular Staining Permeabilization Wash Buffer (BioLegend), and subsequently stained with fluorescein isothiocyanate (FITC)–conjugated anti-EZH2 (clone REA907; Miltenyi Biotec) or with corresponding isotype control, REA Control (I) antibody (clone REA293; Miltenyi Biotec). Stained cells were then analyzed by flow cytometry using an iCyt Synergy SY3200 Cell Sorter (Sony Biotechnology) and FlowJo software, version 10.0.7. An example of the gating strategy to determine B cells, monocytes, and neutrophils is shown in Supplementary Figure 1 (http://onlinelibrary.wiley.com/doi/10.1002/art.40931/abstract), based on forward scatter (FSC) versus side scatter (SSC) and positive expression of their respective markers. The expression of EZH2 was measured by the median fluorescence intensity (MFI) of EZH2 antibody minus the MFI of its isotype control.

GEO data analysis. Analysis of EZH2 messenger RNA (mRNA) expression levels between lupus patients and healthy controls (in whole blood cells, CD4+ T cells, and CD19+ B cells) was performed using data sets downloaded from the GEO database (accession nos. GSE72509 and GDS4185). These data sets have previously been described in detail (11,12).

Mice and treatments. Eight-week-old female MRL/*lpr* mice (no. 000485; The Jackson Laboratory) were acclimatized for 2 weeks prior to study commencement and maintained in pathogen-free conditions. There were 2 model types in which DZNep (Cayman Chemical) was administered: a preventative model (DZNep/DZNep) with DZNep treatments that began on day 0 of the study in 10-week-old mice and a therapeutic treatment model (vehicle/DZNep) with DZNep treatments that began on day 28 of the study in 14-week-old mice. A vehicle-only group was also included as control. Mice were treated with either vehicle or DZNep (2 mg/kg) by intraperitoneal injection. DZNep was solubilized in DMSO and diluted in phosphate buffered saline (PBS) prior to injection (final DMSO concentration in PBS was 10%). In the vehicle control group, mice received daily injections of vehicle control for 35 days and were switched to biweekly (Monday and Thursday) dosing until day 98. A similar regimen was used in the DZNep/DZNep prevention model group, in which mice received DZNep once daily from day 0 to day 35 and were then switched to twice-weekly dosing for the remainder of the study. In the vehicle/DZNep therapeutic treatment group, animals received vehicle once daily from day 0 to day 27. On day 28, mice in this group were switched to a daily dose of DZNep until day 63; from day 64 onward, the dosing frequency changed to twice weekly. Animals were monitored and weighed daily throughout the study. This study was performed at Biomodels, an AAALAC-accredited facility, and approved by the Biomodels Institutional Animal Care and Use Committee.

Assessment of lupus nephritis and kidney damage. Kidneys were harvested on day 98 of the study, fixed in formalin, and sections were cut and stained with either hematoxylin and eosin or periodic acid–Schiff (PAS). Glomerulonephritis, crescent formation, and necrosis in kidneys were scored clinically by a pathologist who was blinded with regard to the experimental group. Approximately 125 glomeruli in each PAS-stained slide were counted. Glomeruli were categorized as having crescents,

fibrinoid necrosis, acute glomerulitis, mesangial hypercellularity, segmental glomerulosclerosis, global glomerulosclerosis, or normal architecture. The presence of pseudothrombi, interstitial nephritis, and arteritis was also noted.

Urine was collected every 2 weeks beginning 2 weeks prior to day 0 of the study. Urine albumin and creatinine concentrations were measured using enzyme-linked immunosorbent assay (ELISA) kits from Alpha Diagnostic and R&D Systems, respectively, and were then used to calculate the urine albumin:creatinine ratio.

Quantification of serum and plasma antibodies. Every 2 weeks, serum was collected by retroorbital bleed using serum separator tubes. On day 98 of the study, plasma was collected from all of the animals, while serum was collected in a portion of the DZNep/DZNep-treated mice and all of the vehicle/DZNep-treated mice. Anti–double-stranded DNA (anti-dsDNA) antibody titers in serum or plasma (day 98 only) were determined using ELISA (Alpha Diagnostic).

Spleen and lymph node weight. Spleen and lymph nodes (submaxillary, thoracic, axillary, renal, and mesenteric) were excised on day 98 of the study, trimmed of extra fat and connective tissue, weighed, and photographed. The average weight of all lymph nodes in each mouse was used to represent the average change in lymph node weight between mouse groups.

Flow cytometric analysis of splenocytes. Each spleen was placed in fluorescence-activated cell sorting buffer (0.5% bovine serum albumin, 2 m*M* EDTA in PBS) and processed into single-cell suspension using a gentleMACS Dissociator. Total spleen cell counts were obtained by counting a fraction of the diluted cells by flow cytometry. Red blood cells were lysed using BD Pharm Lyse lysis buffer (BD Biosciences) prior to the addition of mouse FcR Blocking Reagent (Miltenyi Biotec). Cells were stained with the following fluorochrome-conjugated antibodies: VioBlue-conjugated CD3ε (clone 17A2; Miltenyi Biotec), APC–Cy7–conjugated rat anti-mouse CD4 (clone GK1.5; BD Biosciences), PE-conjugated rat anti-mouse CD8a (clone 53-6.7; BD Biosciences), PerCP–Cy5.5–conjugated anti-mouse T cell receptor β chain (TCRβ) (clone H57-597; BioLegend), FITC-conjugated anti-mouse CD19 (clone 6D5; BioLegend), APC-conjugated CD45R (B220) (clone RA3-6B2; Miltenyi Biotec), and PE–Cy7–

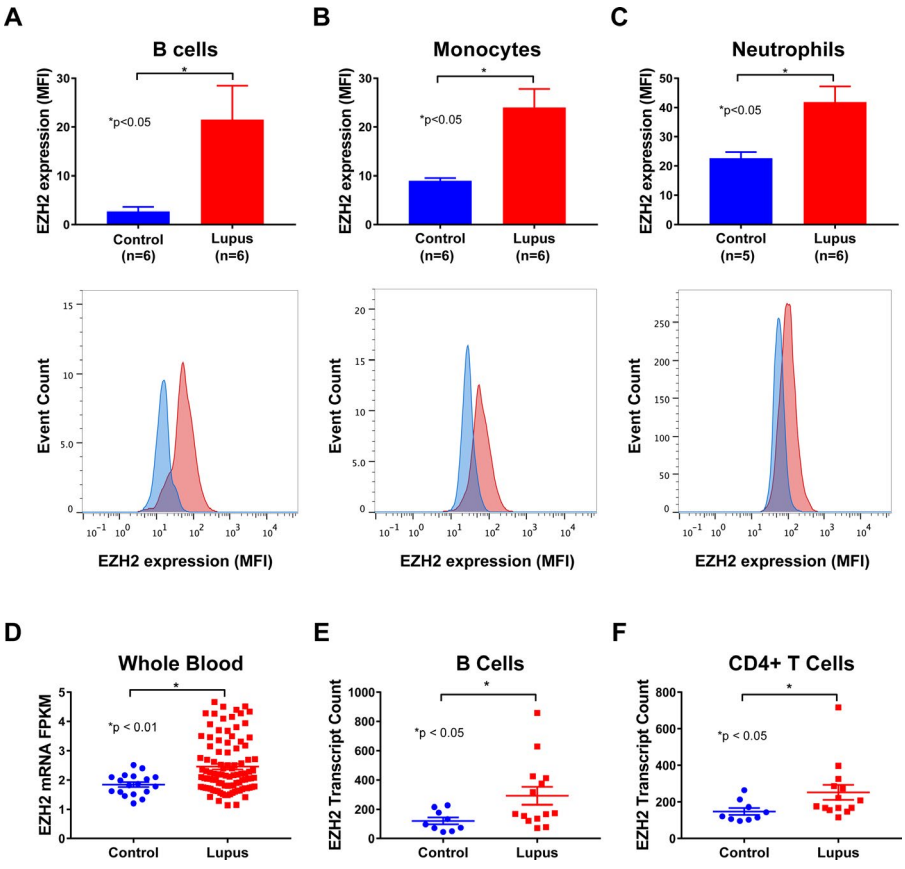

Figure 1. Analysis of EZH2 expression in human peripheral blood cells. **A–C,** EZH2 expression, analyzed by flow cytometry, was elevated in B cells (**A**), monocytes (**B**), and neutrophils (**C**) from lupus patients compared to controls. Values in the upper panels are the mean ± SEM. **D–F,** EZH2 mRNA levels were elevated in whole blood from lupus patients (n = 99) compared to controls (n = 18) (**D**), and were also elevated in B cells (**E**) and CD4+ T cells (**F**) from lupus patients (n = 14) compared to controls (n = 9). Symbols represent individual subjects; bars show the mean ± SEM. MFI = median fluorescence intensity.

conjugated anti-mouse CD11c (clone N418; BioLegend). Stained cells were then analyzed by flow cytometry using a MACSQuant Analyzer 10 (Miltenyi Biotec) and WinList software, version 9 (Verity Software House). The following cell types were gated based on FSC versus SSC and positive expression of their respective markers: B cells (TCRβ–CD19+), total T cells (TCRβ+), CD4+ T cells (TCRβ+CD4+), CD8+ T cells (TCRβ+CD8+), and double-negative T cells (TCRβ+CD4–CD8–). An example of the gating strategy is shown in Supplementary Figure 2 (http://onlinelibrary.wiley.com/doi/10.1002/art.40931/abstract).

EZH2, H3K27me3, and JAM-A expression in splenocytes. To confirm that successful inhibition of EZH2 in mice was achieved by DZNep treatment, EZH2 and H3K27me3 levels in splenocytes were examined using Western blotting. Protein (20 μg) of protein was separated by sodium dodecyl sulfate–polyacrylamide gel electrophoresis before electroblotting onto a nitrocellulose membrane. Blots were probed with anti-EZH2 or anti-H3K27me3 antibodies (both from Cell Signaling Technology). β-actin (Sigma-Aldrich) and H3 (Cell Signaling Technology) were used as loading controls. Since we previously showed that JAM-A is regulated by EZH2 and down-regulated by DZNep in lupus CD4+ T cells (6), we also examined levels of JAM-A (Santa Cruz Biotechnology) in these cells. Densitometry was analyzed using ImageJ.

Cytokine analysis. Cytokine levels in plasma from day 98 of the mouse study were analyzed using a Bio-Plex Pro Mouse Cytokine 23-plex Assay. The cytokines assayed included tumor necrosis factor (TNF), interferon-γ (IFNγ), interleukin-1α (IL-1α), IL-1β, IL-2, IL-3, IL-4, IL-5, IL-6, IL-9, IL-10, IL-12, IL-12p40, IL-13, IL-17A, CCL2, RANTES/CCL5, keratinocyte-derived chemokine (KC)/CXCL1, eotaxin/CCL11, macrophage inflammatory protein 1α (MIP-1α), MIP-1β/CCL4, granulocyte colony-stimulating factor (G-CSF), and granulocyte–macrophage colony-stimulating factor (GM-CSF).

Statistical analysis. Mann-Whitney U tests were used to compare the publicly available data on human EZH2 expression levels in whole blood, B cells, and CD4+ T cells in lupus patients and healthy controls. EZH2 expression , measured by flow cytometry, in B cells, monocytes, and neutrophils from lupus patients versus healthy controls was compared using an

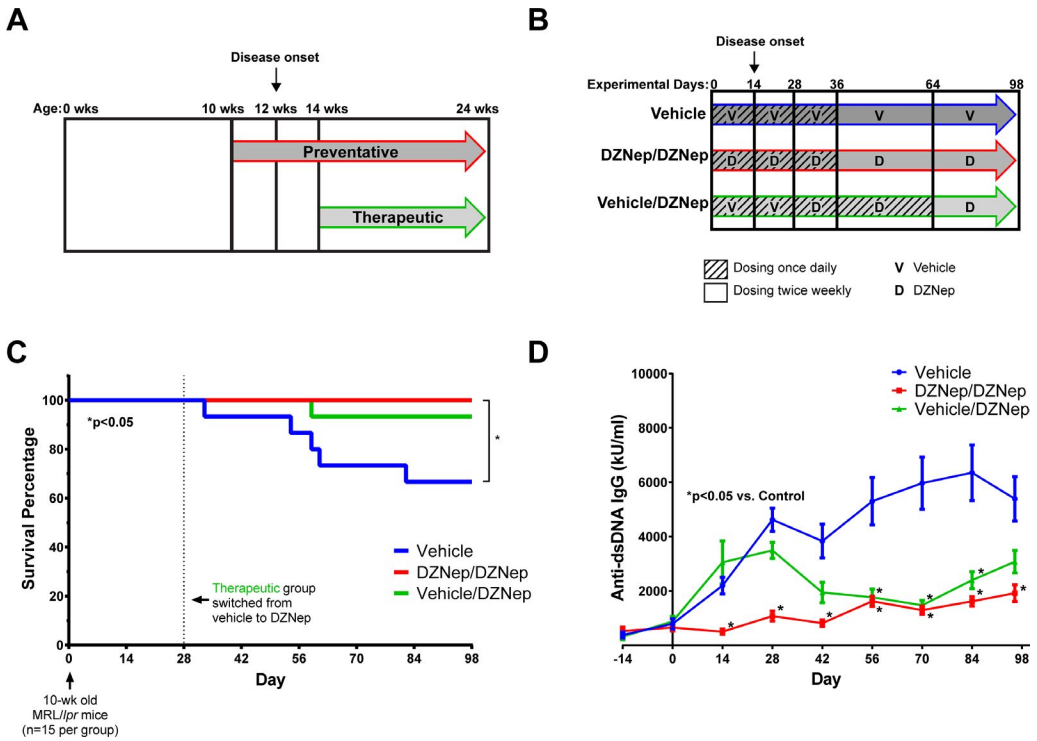

Figure 2. Survival improvement and reduced anti–double-stranded DNA (anti-dsDNA) antibody production in 3′-deazaneplanocin (DZNep)–treated MRL/*lpr* mice. **A**, Schematic representation of preventative and therapeutic treatment models. DZNep treatment in the preventative group (DZNep/DZNep) began when mice were 10 weeks old, 2 weeks prior to typical disease onset. The therapeutic group (vehicle/DZNep) received DZNep treatment 2 weeks after disease onset, when mice were 14 weeks old. **B**, Schematic representation of treatment regimens. The DZNep/DZNep group received DZNep once daily for 35 days and on day 36 was switched to a twice-weekly regimen until the end of the study. The control group was treated at the same times as the DZNep/DZNep group, with vehicle administered instead of DZNep. The vehicle/DZNep group received vehicle once daily for 27 days, then was switched to daily dosing of DZNep from day 28 through day 63. On day 64, DZNep dosing was reduced to twice weekly until the end of the study. **C**, Survival curves of the vehicle, DZNep/DZNep, and vehicle/DZNep groups (n = 15 per group at start). **D**, Anti-dsDNA antibody levels. Values are the mean ± SEM.

unpaired *t*-test, or Mann-Whitney U test when normality could not be assumed. Survival analysis was performed using the Mantel-Cox log-rank test. All other mouse data were evaluated by one-way analysis of variance, or Kruskal-Wallis test when normality could not be assumed, using Dunn's multiple comparison test to compare the preventative and therapeutic groups to the control group. All statistical analyses were performed using GraphPad Prism, version 7. Data are presented as the mean ± SEM. *P* values less than 0.05 were considered significant.

RESULTS

EZH2 expression in lupus. We previously showed that EZH2 is up-regulated in lupus CD4+ T cells and that T cell overexpression of EZH2 plays an important role in lupus (5,6). To examine whether other immune cell types also overexpress EZH2 in lupus, we assessed EZH2 expression using flow cytometry in peripheral blood B cells, monocytes, and neutrophils from lupus patients and compared it to that in healthy controls. EZH2 expression, as measured by MFI, was significantly elevated in B cells, monocytes, and neutrophils of lupus patients compared to matched controls ($P < 0.05$) (Figures 1A–C). Using previously published gene expression profiles available in GEO, we analyzed EZH2 mRNA levels in whole blood (GEO accession no. GSE72509) and freshly isolated lymphocyte subsets (GEO accession no. GDS4185) from lupus patients and healthy controls. EZH2 mRNA levels in whole blood from lupus patients were significantly higher than those in healthy controls ($P < 0.01$) (Figure 1D). Similarly, EZH2 expression was significantly elevated in the freshly isolated B cells and CD4+ T cells from lupus patients compared to controls ($P < 0.05$) (Figures 1E and F).

Effect of EZH2 inhibition on mortality and autoantibody production in MRL/*lpr* mice. To examine whether inhibition of EZH2 is beneficial in lupus-like disease, an EZH2 inhibitor, DZNep, was administered to MRL/*lpr* mice (Figures 2A and B). As shown in Figure 2C, mice that received only vehicle had 33.3% mortality by the end of the study on day 98 (mice were 24 weeks old). Mice in the preventative group had 100% survival, while there was 6.67% mortality in the therapeutic group by the end of the study. There was a significant difference in the mortality rates between the DZNep/DZNep-treated mice and the controls ($P < 0.05$).

Anti-dsDNA antibody levels were significantly lower in the preventative group by day 14, 2 weeks after DZNep treatment began in this group, and anti-dsDNA antibody levels remained significantly lower throughout the duration of the study ($P < 0.001$) (Figure 2D). By day 56, the anti-dsDNA titers were significantly lower in mice in the therapeutic group compared to the vehicle control group ($P < 0.05$) and remained significantly lower for the next 28 days, though there was not a significant difference detected at the final time point (Figure 2D). Although plasma was used instead of serum for quantification of anti-

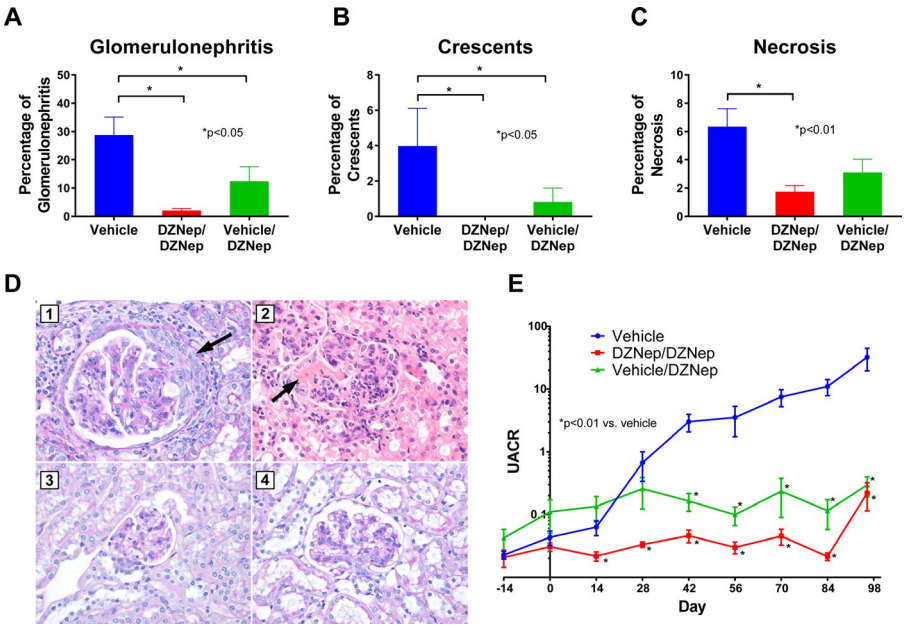

Figure 3. Reduced renal involvement in 3′-deazaneplanocin (DZNep)–treated MRL/*lpr* mice. **A–C,** The percentage of total glomeruli with glomerulonephritis (**A**), crescent formation (**B**), and necrosis (**C**) in the kidneys of mice in the vehicle, DZNep/DZNep, and vehicle/DZNep groups. **D**, Photomicrographic representation of renal damage. D1, Glomerulus with glomerulomegaly and cellular crescent (**arrow**) from a mouse in the control group. D2, Acute global glomerulitis and segmental fibrinoid necrosis (**arrow**) from a mouse in the control group. D3, Normal-appearing glomerulus from a mouse in the DZNep/DZNep group. D4, Glomerulus with mesangial hypercellularity from a mouse in the vehicle/DZNep group. Periodic acid–Schiff stained (D1, D3, and D4) or hematoxylin and eosin stained (D2); original magnification × 400. **E**, Urine albumin:creatinine ratios (UACRs) in the vehicle, DZNep/DZNep, and vehicle/DZNep groups. Values in **A**, **B**, **C**, and **E** are the mean ± SEM.

dsDNA on day 98, the levels were similar to those measured in serum (data not shown). Our results showed that DZNep improved survival in the MRL/*lpr* mice and significantly reduced the production of anti-dsDNA antibodies 2–4 weeks following daily dosing of DZNep.

Effect of DZNep treatment on renal involvement. To assess the effect of DZNep on renal damage, glomerulonephritis, crescent formation, and necrosis were assessed in each mouse on day 98 of the study. Development of glomerulonephritis and crescents was significantly reduced in both the preventative and therapeutic groups compared to the control group ($P < 0.05$) (Figures 3A and B). There also was a significant reduction in glomerular necrosis in the preventative group compared to the control group ($P < 0.01$), but the difference observed between the control group and the therapeutic group was not statistically significant (Figure 3C). Representative photomicrographs of glomeruli from each treatment group are depicted in Figure 3D. Overall, the number of glomeruli with no pathologic abnormality was significantly higher in the preventative group compared to the control group (mean ± SEM 65.8 ± 4.7% versus 31.6 ± 7.2%; $P < 0.01$) (Supplementary Figure 3, http://onlinelibrary.wiley.com/

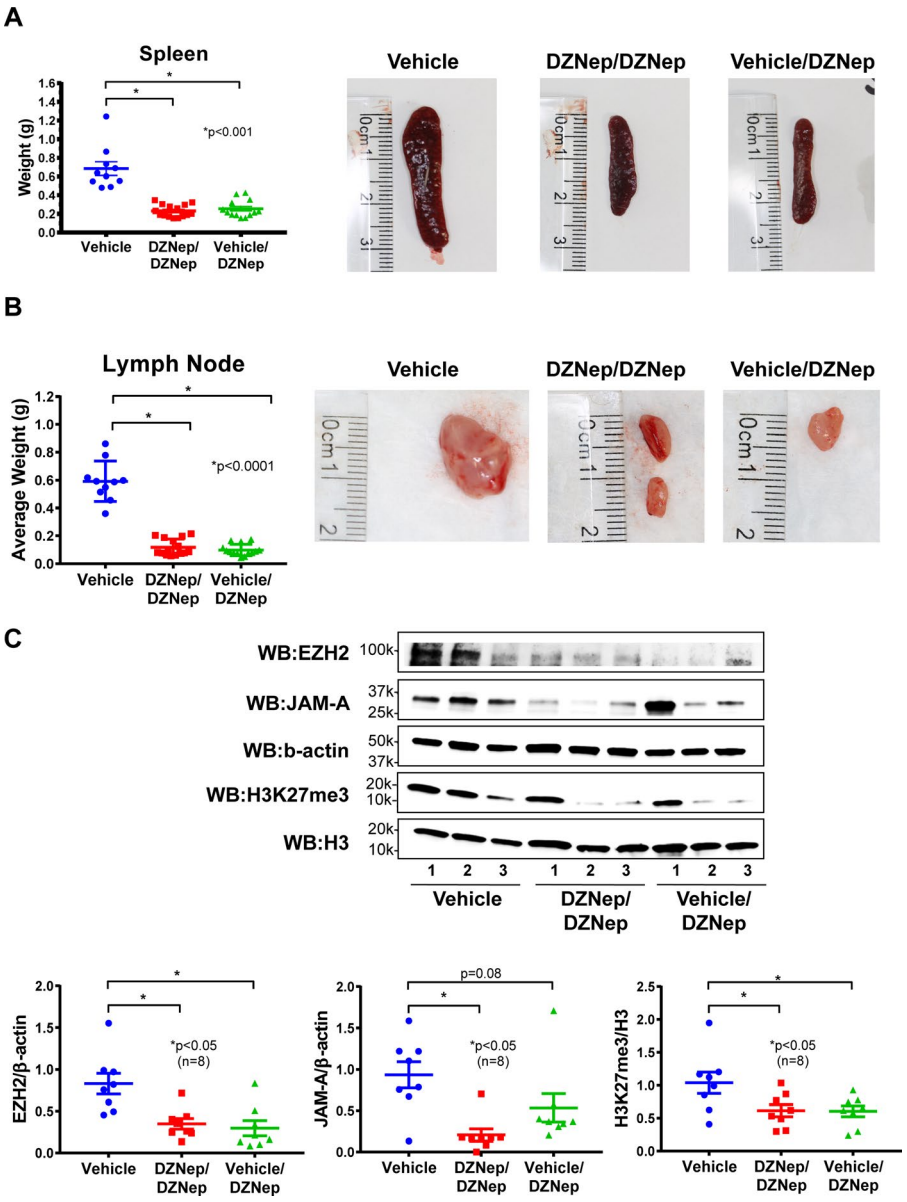

Figure 4. Reduced splenomegaly and lymphadenopathy in 3′-deazaneplanocin (DZNep)–treated MRL/*lpr* mice. **A**, Weight of individual spleens, and representative photographs. **B**, Mean weight of lymph nodes from all sites, and representative photographs of renal lymph nodes. **C**, Expression of EZH2, junctional adhesion molecule A (JAM-A), and H3K27me3 in splenocytes, examined by Western blotting (WB). Representative blots from 3 mice per treatment group are shown. A total of 8 samples per group were analyzed for densitometry. In **A** and **B** (left panels) and **C** (lower panels), symbols represent individual mice; bars show the mean ± SEM.

doi/10.1002/art.40931/abstract). To monitor the progression of kidney involvement, proteinuria was analyzed using albumin:creatinine ratios that were calculated every 2 weeks throughout the study. These ratios were significantly lower in the preventative group (by day 14) and the therapeutic group (by day 42) compared to the control group ($P < 0.01$) (Figure 3E). In both treatment groups, the albumin:creatinine ratio remained significantly lower throughout the remainder of the study. Overall, DZNep treatment, both preventative and therapeutic, significantly reduced lupus nephritis and renal damage in MRL/*lpr* lupus-prone mice.

Reduced splenomegaly and lymphadenopathy with DZNep. MRL/*lpr* mice develop progressive enlargement of the spleen and lymph nodes due to lymphoproliferation that is characteristic of the strain. The spleens from vehicle-treated mice weighed significantly more than those from mice in the preventative and therapeutic groups ($P < 0.001$) (Figure 4A). The mean weight of lymph nodes from all sites (submaxillary, thoracic, axillary, renal, and mesenteric) in both the preventative and therapeutic groups was significantly lower than that of the control group ($P < 0.0001$) (Figure 4B and Supplementary Figure 4, http://onlinelibrary.wiley.com/doi/10.1002/art.40931/abstract). DZNep appeared to be efficacious in reducing the progression of splenomegaly and lymphadenopathy in MRL/*lpr* mice.

Reduced EZH2, H3K27me3, and JAM-A with DZNep. In splenocytes, DZNep treatment in both the preventative and therapeutic groups significantly reduced both EZH2 and H3K27me3 levels, suggesting that the dosing regimen we adopted was effective in inhibiting EZH2 ($P < 0.05$; n = 8) (Figure 4C). In addition, JAM-A levels in splenocytes were significantly reduced in the preventative group ($P < 0.05$), while these reductions were only marginally significant in the therapeutic group due to an outlier ($P = 0.08$). These results suggest that EZH2 regulates JAM-A expression, and manipulation of EZH2 expression by DZNep down-regulates JAM-A, similar to what we previously showed in CD4+ T cells in lupus patients (6).

Reduced lymphoproliferation with DZNep. Using flow cytometry, we further explored the effect of EZH2 inhibition on lymphoproliferation in MRL/*lpr* mice by analyzing differences between groups of T cell and B cell populations. Both the preventative and therapeutic groups showed reduced numbers of total splenocytes, total T cells (TCRβ+), CD8+ T cells (TCRβ+CD8+), and double-negative T cells (TCRβ+CD4–CD8–), compared to the control group ($P < 0.01$) (Figures 5A–C). The total number of CD4+ T cells (TCRβ+CD4+) was significantly decreased in the therapeutic group compared to the control group ($P < 0.01$) (Figure 5C). In addition, DZNep treatment in both the preventative and therapeutic groups significantly reduced the percentage of double-negative T cells, while significantly increasing the percentage of CD4+ and CD8+ T cells by the end of the study, compared to the control group ($P \leq 0.0001$) (Figure 5D). The observed shift in T cell populations and the reduction in total number of T cells suggests that DZNep reduces both T cell hyperproliferation and the generation of pathogenic double-negative T cells in MRL/*lpr* mice.

There was no difference in the total number of B cells (TCRβ–CD19+) between any of the groups (Figure 5E). However, we observed that the B cell percentage among total splenocytes was significantly greater in both the preventative and therapeutic groups compared to the control group ($P \leq 0.0001$) (Figure 5F).

Cytokine levels. To further characterize the effect of EZH2 inhibition in MRL/*lpr* mice, we analyzed the differential expression of plasma cytokine levels on day 98. Levels of IL-3, IL-1β, IL-9, IL-13, IL-6, IL-4, G-CSF, GM-CSF, and MIP-1α were undetectable. No significant differences were observed between DZNep treatment groups and controls for IL-2, IL-5, IL-1α, IL-17A, and eotaxin/CCL11 (data not shown). However, there was a signifi-

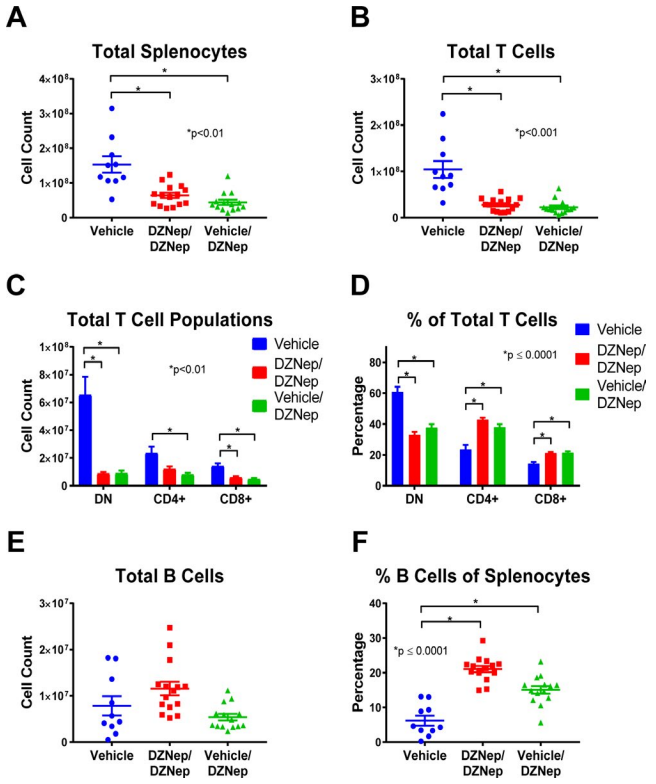

Figure 5. Reduced lymphoproliferation in 3′-deazaneplanocin (DZNep)–treated MRL/*lpr* mice. **A** and **B**, Total numbers of splenocytes (**A**) and T cells (**B**) in the DZNep/DZNep and vehicle/DZNep groups compared to controls. **C** and **D**, Total numbers (**C**) and percentages (**D**) of double-negative (DN) T cells, CD4+ T cells, and CD8+ T cells in mice in each treatment group. Values are the mean ± SEM. **E** and **F**, Total numbers of B cells (**E**) and percentages of B cells among splenocytes (**F**) in mice in each treatment group. In **A**, **B**, **E**, and **F**, symbols represent individual mice; bars show the mean ± SEM.

cant reduction in plasma levels of TNF, IFNγ, CCL2, RANTES/CCL5, IL-10, KC/CXCL1, IL-12, IL-12p40, and MIP-1β/CCL4 in both the preventative and therapeutic groups compared to the control group (Figure 6).

DISCUSSION

Our previous findings suggested that EZH2 plays an important role in lupus (5,6). We have reported that naive CD4+ T cells in lupus patients showed higher expression levels of EZH2 than those in healthy controls, and this up-regulation is critical for T cell adhesion, as inhibition of EZH2 by DZNep can normalize the ability of lupus CD4+ T cells to adhere to endothelial cells (6). In the present study, we further examined the expression of EZH2 in other cell types and showed that EZH2 was significantly up-regulated in B cells, monocytes, and neutrophils in lupus patients. These data prompted us to investigate whether inhibition of EZH2 would be beneficial for lupus treatment. Indeed, in MRL/*lpr* mice, DZNep treatment, administered in either a preventative or a therapeutic protocol, improved survival and reduced autoantibody production. In addition, the therapeutic effects of DZNep appeared rapidly, with lowered anti-dsDNA antibody levels and albumin:creatinine ratio evident 14 days after the first dose.

The improvement in survival observed in DZNep-treated mice is likely due, in part, to a reduction in renal involvement. DZNep treatments appeared to prevent the progression of renal damage, as evidenced by a relatively stable albumin:creatinine ratio in DZNep-treated mice. Renal damage was also assessed at the end of the study by histopathologic examination. We observed a significant reduction in glomerulonephritis and crescent formation in both DZNep treatment groups and a significant reduction in glomerular necrosis in the preventative group (DZNep/DZNep) compared to the control group, by the end of the study. The development of nephritis is indicative of severe disease in lupus patients and is an important predictor of morbidity and mortality. Based on our finding that DZNep treatment effectively reduced renal involvement in MRL/*lpr* mice, an EZH2 inhibitor could prove similarly therapeutic for lupus patients.

The MRL/*lpr* mouse model is a lymphoproliferative model characterized by T cell and B cell dysregulation (13). The infiltration of double-negative T cells, in addition to an overall hyperproliferation of T cell populations, contributes significantly to the

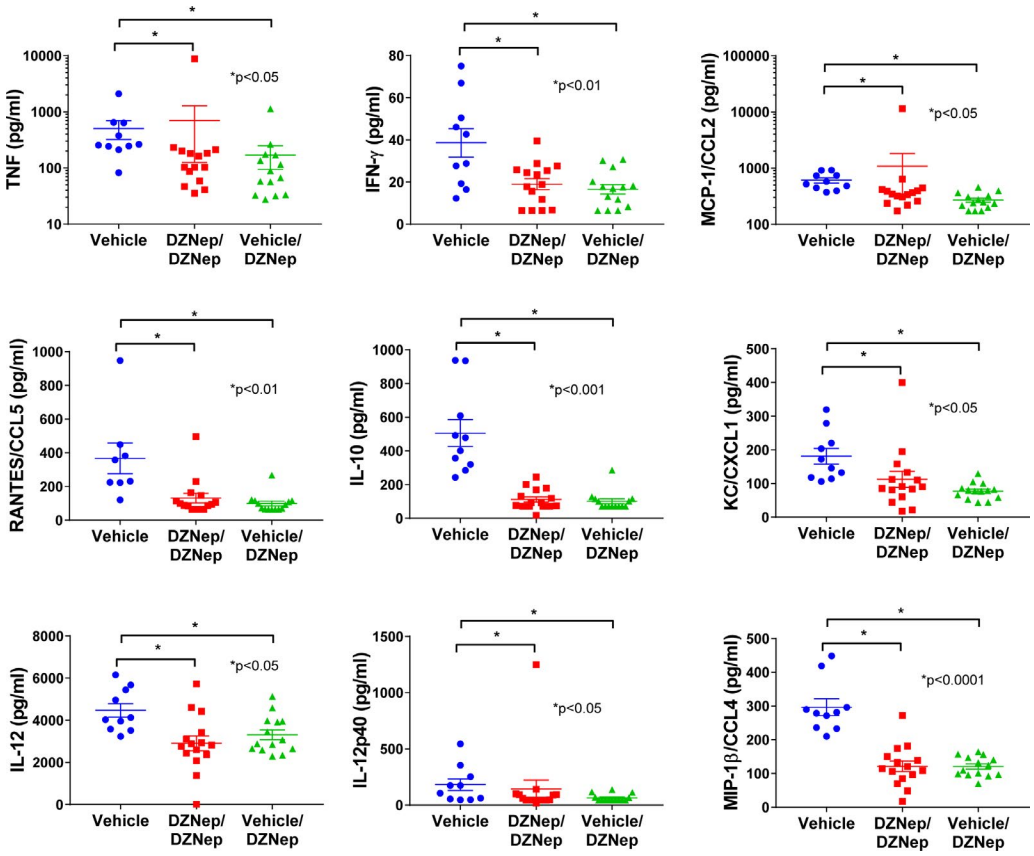

Figure 6. Decreased levels of plasma cytokines in 3′-deazaneplanocin (DZNep)–treated MRL/*lpr* mice. There was a significant reduction in plasma levels of tumor necrosis factor (TNF), interferon-γ (IFNγ), monocyte chemotactic protein 1 (MCP-1)/CCL2, RANTES/CCL5, interleukin-10 (IL-10), keratinocyte-derived chemokine (KC)/CXCL1, IL-12, IL-12p40, and macrophage inflammatory protein 1β (MIP-1β)/CCL4 in both the DZNep/DZNep and vehicle/DZNep groups compared to the control group. Symbols represent individual mice; bars show the mean ± SEM.

observed splenomegaly and lymphadenopathy in MRL/*lpr* mice (13,14). We observed a significant reduction in spleen and lymph node weight in both groups of mice treated with DZNep. A significant decrease in the total number of splenocytes in DZNep-treated groups was also observed, suggesting a reduction in lymphoproliferation. While DZNep treatment in both groups reduced the total number of T cells, CD4+ T cells, and CD8+ T cells, the reduction in CD4−CD8− (double-negative) T cells is of particular interest. Double-negative T cells represent a pathogenic T cell subset in lupus likely derived from CD8+ T cells (15). These cells contribute to the production of autoantibodies, produce significant amounts of inflammatory cytokines including IL-17 and IFNγ, and contribute to renal damage as they accumulate in the kidneys of lupus patients (15–18). Inhibition of EZH2 with DZNep significantly reduced the total number of pathogenic double-negative T cells in MRL/*lpr* mice. Indeed, the significant reduction in double-negative T cell numbers observed with DZNep treatment caused significant elevation in the percentages of single-positive T cells (CD4+ and CD8+ T cells). We speculate that the reduction of pathogenic double-negative T cells in the DZNep-treated groups likely contributed to the observed reduction in renal damage and levels of circulating autoantibodies.

Production of cytokines and chemokines is important in lupus pathogenesis and tissue damage in lupus patients. We observed reduced concentrations of TNF, IFNγ, CCL2, RANTES/CCL5, IL-10, IL-12, IL-12p40, and MIP-1β/CCL4 in the plasma from mice in the DZNep-treated groups compared to controls. All of these cytokines and chemokines have been reported to be elevated in lupus patients (19–23). Chemokines such as RANTES/CCL5, monocyte chemotactic protein 1/CCL2, and MIP-1β/CCL4 contribute to lupus pathogenesis by recruiting leukocytes and other effector cells to inflamed tissues, causing damage (19–21). IL-10 and TNF have been shown to be up-regulated in lupus patients experiencing renal involvement, and their levels correlate with disease activity (19,22). IFNγ has been found to contribute to the development of lupus through promotion of autophagy in lupus T cells, and potentially the persistence of pathogenic T cell subsets (22). Dysregulation of IL-12 has been reported in patients with lupus (24), and promising results were seen in a recent phase II trial in which ustekinumab, which targets IL-12p40, was added to the standard of care in lupus patients (25).

We have previously demonstrated that EZH2 might mediate a pathogenic effect in lupus by altering T cell DNA methylation patterns and up-regulation of the adhesion molecule JAM-A in CD4+ T cells (5,6). In the present study, we showed that DZNep treatment in MRL/*lpr* mice also down-regulates JAM-A in splenocytes, suggesting that its beneficial effect in these animals might be due, in part, to inhibition of lymphocyte adhesion and extravasation. Because the Notch signaling pathway regulates effector T cell survival and function, including cytokine production (26–28), we speculated that another potential mechanism of action for EZH2 in lupus might involve the Notch signaling pathway. EZH2 has been shown to inhibit T cell Notch repressors, promoting Notch activation and thus effector T cell polyfunctionality and survival (29). The Notch pathway is also critical in B cells and monocytes (30–34), which were characterized by EZH2 overexpression in lupus in our study.

Several limitations to this study are worth noting. We utilized a systemic approach to inhibit EZH2. While this approach allowed for assessment of the overall effect of EZH2 inhibition (which would be important if a clinical trial using EZH2 inhibitors were to be conducted in lupus patients), it did not allow for the identification of the specific cell types or pathways mediating the therapeutic effect of EZH2 inhibition in this lupus-prone mouse model. In addition, as noted above, although DZNep is a prototype EZH2 inhibitor, it inhibits methyltransferase activity, and therefore, nonspecific effects of DZNep cannot be ruled out. Future studies focused on characterizing the effects of EZH2 inhibition in specific cell types in vivo and on utilizing other more specific EZH2 inhibitors are warranted.

In summary, we have demonstrated that EZH2 is overexpressed in multiple immune cell types in lupus patients. Inhibition of EZH2 is associated with abrogation of lupus-like disease in MRL/*lpr* mice. Our data suggest that inhibiting EZH2 might provide a novel therapeutic approach for lupus patients.

AUTHOR CONTRIBUTIONS

All authors were involved in drafting the article or revising it critically for important intellectual content, and all authors approved the final version to be published. Dr. Sawalha had full access to all of the data in the study and takes responsibility for the integrity of the data and the accuracy of the data analysis.

Study conception and design. Tsou, Sawalha.
Acquisition of data. Rohraff, He, Schonfeld, Tsou, Sawalha.
Analysis and interpretation of data. Rohraff, Farkash, Tsou, Sawalha.

REFERENCES

1. Weeding E, Sawalha AH. Deoxyribonucleic acid methylation in systemic lupus erythematosus: implications for future clinical practice. Front Immunol 2018;9:875.
2. Deng Y, Tsao BP. Updates in lupus genetics. Curr Rheumatol Rep 2017;19:68.
3. Hedrich CM. Mechanistic aspects of epigenetic dysregulation in SLE. Clin Immunol 2018;196:3–11.
4. Teruel M, Sawalha AH. Epigenetic variability in systemic lupus erythematosus: what we learned from genome-wide DNA methylation studies. Curr Rheumatol Rep 2017;19:32.
5. Coit P, Dozmorov MG, Merrill JT, McCune WJ, Maksimowicz-McKinnon K, Wren JD, et al. Epigenetic reprogramming in naive CD4+ T cells favoring T cell activation and non-Th1 effector T cell immune response as an early event in lupus flares. Arthritis Rheumatol 2016;68:2200–9.
6. Tsou PS, Coit P, Kilian NC, Sawalha AH. EZH2 modulates the DNA methylome and controls T cell adhesion through junctional adhesion molecule A in lupus patients. Arthritis Rheumatol 2018;70:98–108.
7. Gan L, Yang Y, Li Q, Feng Y, Liu T, Guo W. Epigenetic regulation of cancer progression by EZH2: from biological insights to therapeutic potential [review]. Biomark Res 2018;6:10.

8. Glazer RI, Hartman KD, Knode MC, Richard MM, Chiang PK, Tseng CK, et al. 3-deazaneplanocin: a new and potent inhibitor of S-adenosylhomocysteine hydrolase and its effects on human promyelocytic leukemia cell line HL-60. Biochem Biophys Res Commun 1986;135:688–94.
9. Hochberg MC, for the Diagnostic and Therapeutic Criteria Committee of the American College of Rheumatology. Updating the American College of Rheumatology revised criteria for the classification of systemic lupus erythematosus [letter]. Arthritis Rheum 1997;40:1725.
10. Bombardier C, Gladman DD, Urowitz MB, Caron D, Chang DH, and the Committee on Prognosis Studies in SLE. Derivation of the SLEDAI: a disease activity index for lupus patients. Arthritis Rheum 1992;35:630–40.
11. Hutcheson J, Scatizzi JC, Siddiqui AM, Haines GK III, Wu T, Li QZ, et al. Combined deficiency of proapoptotic regulators Bim and Fas results in the early onset of systemic autoimmunity. Immunity 2008;28:206–17.
12. Hung T, Pratt GA, Sundararaman B, Townsend MJ, Chaivorapol C, Bhangale T, et al. The Ro60 autoantigen binds endogenous retroelements and regulates inflammatory gene expression. Science 2015;350:455–9.
13. Cohen PL, Eisenberg RA. Lpr and gld: single gene models of systemic autoimmunity and lymphoproliferative disease. Annu Rev Immunol 1991;9:243–69.
14. Lu LD, Stump KL, Wallace NH, Dobrzanski P, Serdikoff C, Gingrich DE, et al. Depletion of autoreactive plasma cells and treatment of lupus nephritis in mice using CEP-33779, a novel, orally active, selective inhibitor of JAK2. J Immunol 2011;187:3840–53.
15. Crispín JC, Tsokos GC. Human TCR-αβ+ CD4– CD8– T cells can derive from CD8+ T cells and display an inflammatory effector phenotype. J Immunol 2009;183:4675–81.
16. Crispín JC, Oukka M, Bayliss G, Cohen RA, Van Beek CA, Stillman IE, et al. Expanded double negative T cells in patients with systemic lupus erythematosus produce IL-17 and infiltrate the kidneys. J Immunol 2008;181:8761–6.
17. Shivakumar S, Tsokos GC, Datta SK. T cell receptor α/β expressing double-negative (CD4-/CD8-) and CD4+ T helper cells in humans augment the production of pathogenic anti-DNA autoantibodies associated with lupus nephritis. J Immunol 1989;143:103–12.
18. Dean GS, Anand A, Blofeld A, Isenberg DA, Lydyard PM. Characterization of CD3+ CD4- CD8- (double negative) T cells in patients with systemic lupus erythematosus: production of IL-4. Lupus 2002;11:501–7.
19. Lit LC, Wong CK, Tam LS, Li EK, Lam CW. Raised plasma concentration and ex vivo production of inflammatory chemokines in patients with systemic lupus erythematosus. Ann Rheum Dis 2006;65:209–15.
20. Vilá LM, Molina MJ, Mayor AM, Cruz JJ, Ríos-Olivares E, Ríos Z. Association of serum MIP-1α, MIP-1β, and RANTES with clinical manifestations, disease activity, and damage accrual in systemic lupus erythematosus. Clin Rheumatol 2007;26:718–22.
21. Kulkarni O, Pawar RD, Purschke W, Eulberg D, Selve N, Buchner K, et al. Spiegelmer inhibition of CCL2/MCP-1 ameliorates lupus nephritis in MRL-(Fas)lpr mice. J Am Soc Nephrol 2007;18: 2350–8.
22. Pacheco-Lugo L, Sáenz-García J, Navarro Quiroz E, González Torres H, Fang L, Díaz-Olmos Y, et al. Plasma cytokines as potential biomarkers of kidney damage in patients with systemic lupus erythematosus. Lupus 2019;28:34–43.
23. Arriens C, Wren JD, Munroe ME, Mohan C. Systemic lupus erythematosus biomarkers: the challenging quest. Rheumatology (Oxford) 2017;56 Suppl 1:i32–45.
24. Tucci M, Lombardi L, Richards HB, Dammacco F, Silvestris F. Overexpression of interleukin-12 and T helper 1 predominance in lupus nephritis. Clin Exp Immunol 2008;154:247–54.
25. Van Vollenhoven RF, Hahn BH, Tsokos GC, Wagner CL, Lipsky P, Touma Z, et al. Efficacy and safety of ustekinumab, an IL-12 and IL-23 inhibitor, in patients with active systemic lupus erythematosus: results of a multicentre, double-blind, phase 2, randomised, controlled study. Lancet 2018;392:1330–9.
26. Amsen D, Blander JM, Lee GR, Tanigaki K, Honjo T, Flavell RA. Instruction of distinct CD4 T helper cell fates by different notch ligands on antigen-presenting cells. Cell 2004;117:515–26.
27. Ciofani M, Zúñiga-Pflücker JC. Notch promotes survival of pre-T cells at the β-selection checkpoint by regulating cellular metabolism. Nat Immunol 2005;6:881–8.
28. Kryczek I, Zhao E, Liu Y, Wang Y, Vatan L, Szeliga W, et al. Human TH17 cells are long-lived effector memory cells. Sci Transl Med 2011;3:104ra100.
29. Zhao E, Maj T, Kryczek I, Li W, Wu K, Zhao L, et al. Cancer mediates effector T cell dysfunction by targeting microRNAs and EZH2 via glycolysis restriction. Nat Immunol 2016;17:95–103.
30. Cruickshank MN, Ulgiati D. The role of notch signaling in the development of a normal B-cell repertoire. Immunol Cell Biol 2010;88:117–24.
31. Arima H, Nishikori M, Otsuka Y, Kishimoto W, Izumi K, Yasuda K, et al. B cells with aberrant activation of Notch1 signaling promote Treg and Th2 cell-dominant T-cell responses via IL-33. Blood Adv 2018;2:2282–95.
32. Zhang W, Xu W, Xiong S. Blockade of Notch1 signaling alleviates murine lupus via blunting macrophage activation and M2b polarization. J Immunol 2010;184:6465–78.
33. Huang F, Zhao JL, Wang L, Gao CC, Liang SQ, An DJ, et al. MiR-148a-3p mediates Notch signaling to promote the differentiation and M1 activation of macrophages. Front Immunol 2017;8:1327.
34. Martín-Gayo E, González-García S, García-León MJ, Murcia-Ceballos A, Alcain J, García-Peydró M, et al. Spatially restricted JAG1-Notch signaling in human thymus provides suitable DC developmental niches. J Exp Med 2017;214:3361–79.